

Supplemental document

Table S1. Model parameters for oxygen transport and consumption at 37 °C.

Description	Parameters	Value	References
Henry's constant for oxygen	K_{H,O_2}	$1.32 \times 10^{-3} \text{ mol}\cdot\text{m}^{-3}\cdot\text{mmHg}^{-1}$	[1]
Oxygen partial pressure in atmosphere	P_{O_2}	159 mmHg	[1,2]
Oxygen concentration in medium entering the system	C_{in,O_2}	0.21 mol/m ³	[3,4]
Oxygen diffusion in medium	D_{O_2}	$3 \times 10^{-9} \text{ m}^2/\text{s}$	[3,4,9]
Oxygen permeability in PDMS	P_{PDMS}	$3.786 \times 10^{-11} \text{ mol}\cdot\text{m}\cdot\text{m}^{-2}\cdot\text{s}^{-1}\cdot\text{mmHg}^{-1}$	[5,6]
Hepatocyte maximum oxygen consumption rate	V_{max,O_2}	$4.8 \times 10^{-17} \text{ mol}\cdot\text{cell}^{-1}\cdot\text{s}^{-1}$	[3,7,8]
Michaelis-Menten constant for hepatocyte oxygen consumption	K_{m,O_2}	0.5 mmHg	[3,8]

Table S2. The primers used for real-time RT-PCR in this study.

Gene Symbol	Primers (forward/reverse; 5' to 3')
CYP1A1	GATGGTCAAGGAGCACTACA/AAAGAGGTCCAAGACGATGT
CYP1A2	TCAATGACATCTTTGGAGCAG/CTCTGTATCTCAGGCTTGGTC
CYP2B6	GGGAGATTGAACAGGTGATTG/GATGATGTACCCTCGGAAGC
CYP2C9	GGATTTGTGTGGGAGAAGC/TGAAGCACAGCTGGTAGAAG
CYP2D6	CGCATCCCTAAGGGAACGACA/CAGGAAGTGTTCGGGGTGGAA
CYP2E1	CCATCAAGGATAGGCAAGAG/TCCAGAGTTGGCACTACGAC
CYP3A4	TGCTCTACCATAAGGGCTT/GGCTGTTGACCATCATAAAAG
CYP3A5	ATATGGGACCCGTACACATG/CAGAGACCCTGACGATAGGAC
UGT1A1	GAATCAACTGCCTTACCAA/GACTGTCTGAGGGATTTTGC
UGT2B4	TGTCTACAGCCTCCGCTTCT/GAACTGATCCCATTCTTCATG
SULT1A1	GAGCCGCACCCACCCTGTT/TGAACGACGTGTGCTGAACCAC
SULT2A1	AAAGACGTTAGAACCCGAAGA/TTTCCAGTCCCAGATACACC
OAT2	GTGATGCTGCTGGCACTGGTT/CTCTTTCACATGGCCTTGGGTC
OCT1	AAGAGGATGTCACCGAAAAGC/GGATGAGCCCCTGATAGAGCA
SLCO1B3	GCCTAACCTTGACCTATGAT/CAGGTAAGTTATTCCATTGTTT
SLCO2B1	GGGAGTCCACGAAGAAGCAG/GACAGGACCACCAGCAGGAA
AHR	GGTTGTGATGCCAAAGGAAGA/TCATTGCGATATGGGACTCG
RXR α	TCGTCTCTTTAACCTGACTC/GCTGCTCTGGGTACTTGTGCT
PXR	GGTCCCAAATCTGCCGTGTA/CCGGGCGTTGCGTTTCATG
CAR	TTGCAGAAGTGCTTAGATGCT/TCAGCTCTTCTGCTCCTTACT
MRP2	GACAATTCTAATCTAGCTACTCC/CATCAACTCCCAGACATCC
BCRP	GTTCTTGGATGAGCCTACA/CTGAGGCCAATAAGGTCA
MDR1	GCTCGTGCCCTTGTTAGAC/GTGCCATGCTCCTTGACTC
BSEP	CCCTCATCCGAAATCCAAGA/TGCAGTGCCATGTTCAAACC
Albumin	ACCCCAAGTGTCAACTCAA/GGTTTCAGGACCACGGATAGA

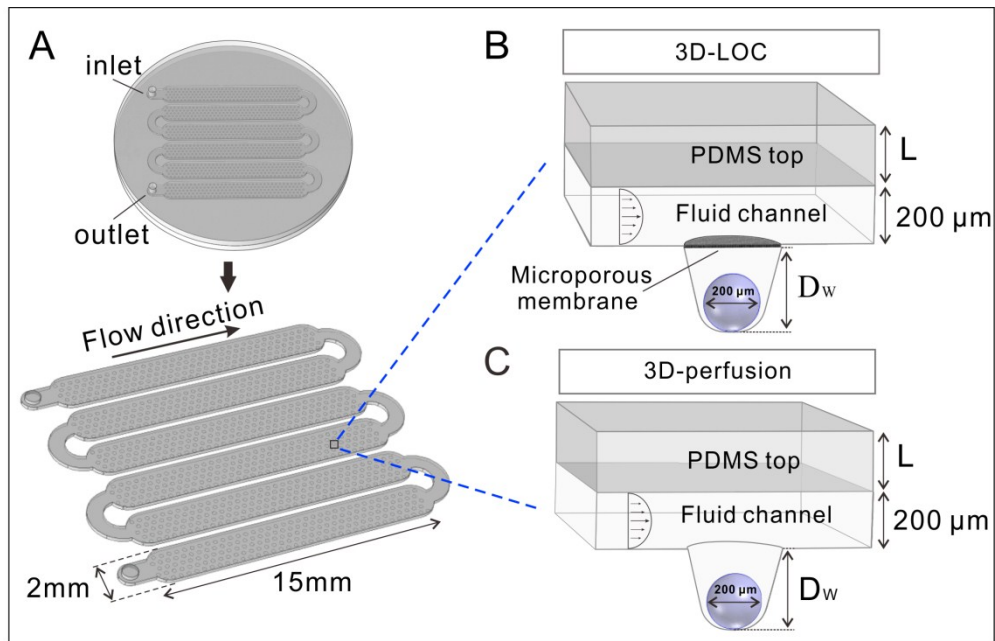


Figure S1. FEM model geometry of the 3D-LOC for the simulation analysis of flow and oxygen mass transfer. (A) 3D geometry of the modeled microfluidic channel, which contained 180×6 arrays of microwells. (B) A single microwell geometry of 3D-LOC, which contained a microporous membrane and a $\text{Ø } 200 \mu\text{m}$ cell spheroid. The microwell had a V-shape cross section with round bottom ($\text{Ø } 250 \mu\text{m} \times 25^\circ$ Angle). The fluid channel height, top PDMS layer thickness and microwell depth were $200 \mu\text{m}$, L and D_w , respectively. (C) For comparison, a single microwell geometry with open microwell (Conventional perfusion method, 3D-perfusion) was also constructed and the dimension parameters were the same as those in (B).

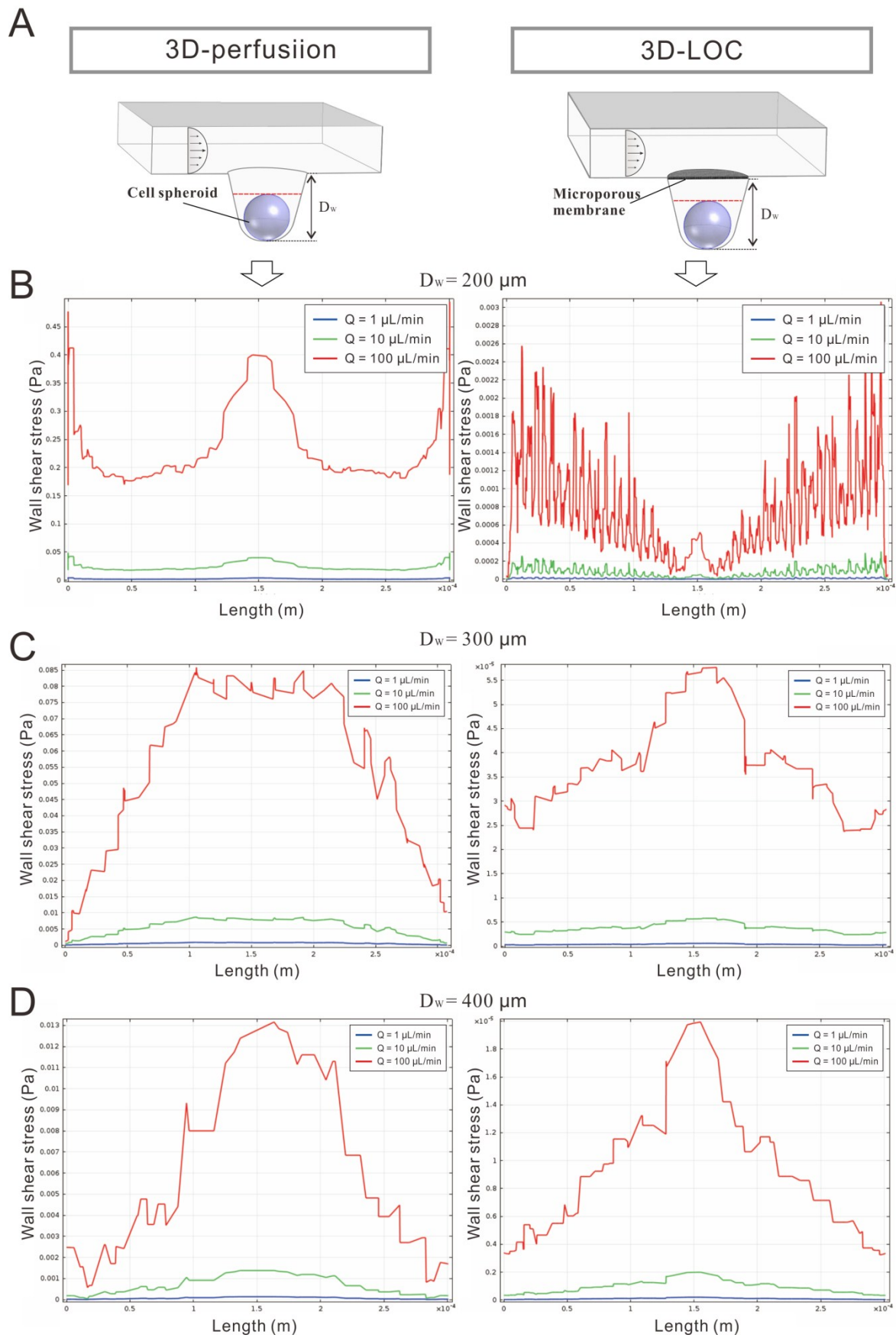


Figure S2. A comparison of wall shear stress in two different perfusion methods (3D-perfusiion and 3D-LOC). The wall shear stress distribution along the top red cut lines of the cell spheroid, described in (A), were plotted in different microwell depth configurations including (B) $D_w = 200 \mu\text{m}$, (C) $D_w = 300 \mu\text{m}$, and (D) $D_w = 400 \mu\text{m}$.

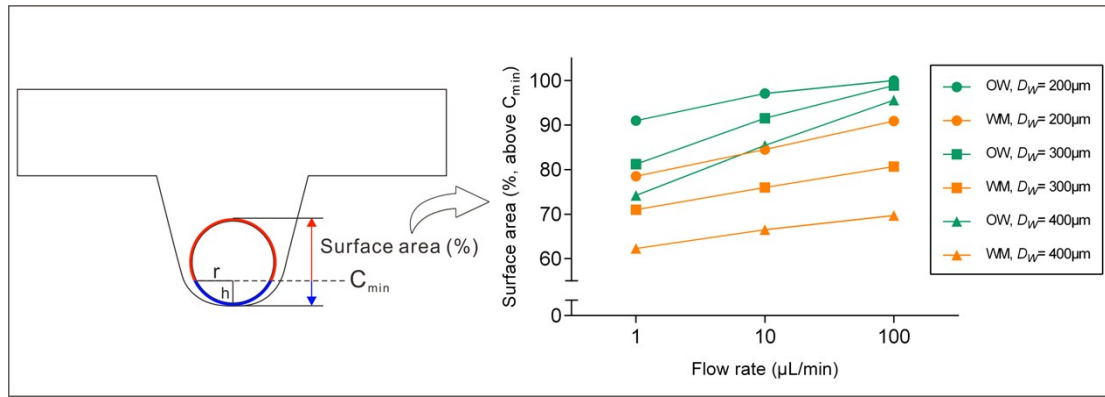


Figure S3. The percentage of the surface area of the cell spheroid (Oxygen concentration $> C_{min}$) in the 3D-perfusion method with open microwell (OW) and in the 3D-LOC method with membrane (MW) at different microwell depths ($D_W = 200, 300$ and $400 \mu\text{m}$) and flow rates ($Q = 1, 10$ and $100 \mu\text{L}/\text{min}$).

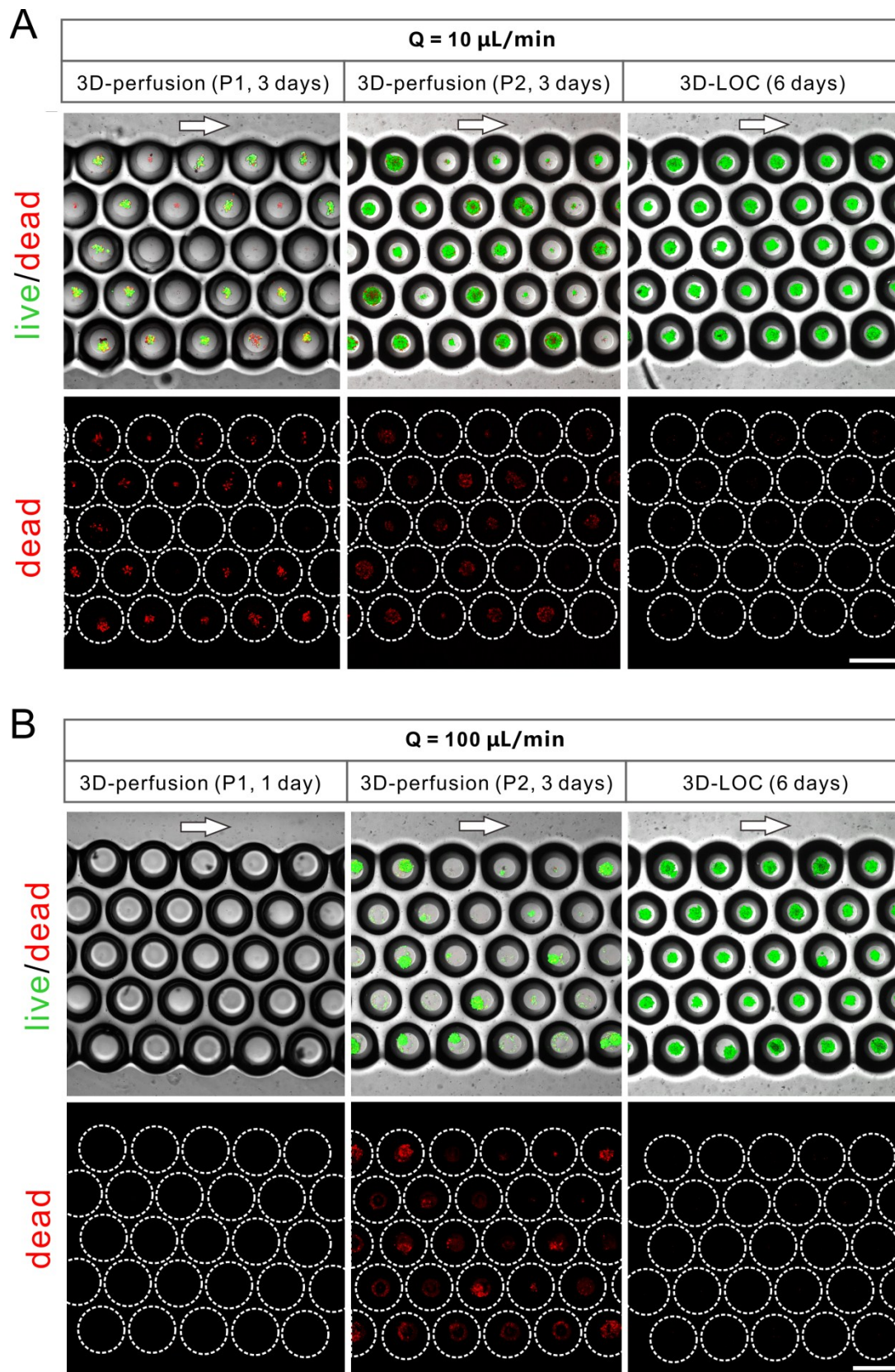


Figure S4. A comparison of cell spheroids viability and loss status in three different perfusion methods (3D-perfusion (P1), 3D-perfusion (P2), and 3D-LOC) perfused cultured for 1-6 days at different flow rates including (A) $Q = 10 \mu\text{L}/\text{min}$, and (B) $Q = 100 \mu\text{L}/\text{min}$. White arrows indicate the direction of fluid flow. Scale bars = 400 μm .

Supplementary References

1. G. Mattei, S. Giusti and A. Ahluwalia, *Processes*, 2014, 2, 548-569.
2. A. R. Frisncho, *Science*, 1975, 187, 313-319.
3. D. Mazzei, M. A. Guzzardi, S. Giusti and A. Ahluwalia, *Biotechnology and bioengineering*, 2010, 106, 127-137.
4. P. Buchwald, *Theoretical biology & medical modelling*, 2011, 8, 20.
5. S. Giulitti, E. Magrofuoco, L. Prevedello and N. Elvassore, *Lab on a chip*, 2013, 13, 4430-4441.
6. E. Cimetta, M. Flaibani, M. Mella, E. Serena, L. Boldrin, P. De Coppi and N. Elvassore, *The International journal of artificial organs*, 2007, 30, 415-428.
7. S. L. Nyberg, R. P. Remmel, H. J. Mann, M. V. Peshwa, W. S. Hu and F. B. Cerra, *Annals of surgery*, 1994, 220, 59-67.
8. J. F. Patzer, 2nd, *Artif Organs*, 2004, 28, 83-98.
9. J. C. Haselgrove, I. M. Shapiro and S. F. Silverton, *The American journal of physiology*, 1993, 265, C497-506.